

Preliminary results on the ^{233}U α -ratio measurement at n_TOF

M. Bacak^{1,2,3,*}, M. Aïche⁴, G. Bélier⁵, E. Berthoumieux³, M. Diakaki^{3,8}, E. Dupont³, F. Gunsing^{3,1}, J. Heyse⁶, S. Kopecky⁶, M. Krčička⁷, B. Laurent⁵, H. Leeb², L. Mathieu⁴, P. Schillebeeckx⁶, O. Serot⁸, J. Taieb⁵, S. Valenta⁷, V. Vlachoudis¹, O. Aberle¹, J. Andrzejewski⁹, L. Audouin¹⁰, J. Balibrea¹¹, M. Barbagallo¹², F. Bečvář⁷, J. Billowes¹³, D. Bosnar¹⁴, A. Brown¹⁵, M. Caamaño¹⁶, F. Calviño¹⁷, M. Calviani¹, D. Cano-Ott¹¹, R. Cardella¹, A. Casanovas¹⁷, F. Cerutti¹, Y. H. Chen¹⁰, E. Chiaveri^{1,13,18}, N. Colonna¹², G. Cortés¹⁷, M. A. Cortés-Giraldo¹⁸, L. Cosentino¹⁹, L. A. Damone^{12,20}, C. Domingo-Pardo²¹, R. Dressler²², I. Durán¹⁶, B. Fernández-Domínguez¹⁶, A. Ferrari¹, P. Ferreira²³, P. Finocchiaro¹⁹, V. Furman²⁴, K. Göbel²⁵, A. R. García¹¹, A. Gawlik⁹, S. Gilardoni¹, T. Glodariu^{†26}, I. F. Gonçalves²³, E. González-Romero¹¹, E. Griesmayer², C. Guerrero¹⁸, H. Harada²⁷, S. Heinitz²², D. G. Jenkins¹⁵, E. Jericha², F. Käppeler²⁸, Y. Kadi¹, A. Kalamara²⁹, P. Kavragin², A. Kimura²⁷, N. Kivel²², I. Knapova⁷, M. Kokkoris²⁹, D. Kurtulgil²⁵, E. Leal-Cidoncha¹⁶, C. Lederer³⁰, J. Lerendegui-Marco¹⁸, S. Lo Meo^{31,32}, S. J. Lonsdale³⁰, D. Macina¹, A. Manna^{32,33}, J. Marganiec^{9,34}, T. Martínez¹¹, A. Masi¹, C. Massimi^{32,33}, P. Mastinu³⁵, M. Mastromarco¹², E. A. Mauger²², A. Mazzone^{12,36}, E. Mendoza¹¹, A. Mengoni³¹, P. M. Milazzo³⁷, F. Mingrone¹, A. Musumarra^{19,38}, A. Negret²⁶, R. Nolte³⁴, A. Oprea²⁶, N. Patronis³⁹, A. Pavlik⁴⁰, J. Perkowski⁹, I. Porras⁴¹, J. Praena⁴¹, J. M. Quesada¹⁸, D. Radeck³⁴, T. Rauscher^{42,43}, R. Reifarth²⁵, C. Rubbia¹, J. A. Ryan¹³, M. Sabaté-Gilarte^{1,18}, A. Saxena⁴⁴, D. Schumann²², P. Sedyshev²⁴, A. G. Smith¹³, N. V. Sosnin¹³, A. Stamatopoulos²⁹, G. Tagliente¹², J. L. Tain²¹, A. Tarifeño-Saldivia¹⁷, L. Tassan-Got¹⁰, G. Vannini^{32,33}, V. Variale¹², P. Vaz²³, A. Ventura³², R. Vlastou²⁹, A. Wallner⁴⁵, S. Warren¹³, C. Weiss², P. J. Woods³⁰, T. Wright¹³, P. Žugec^{14,1}, and the n_TOF Collaboration¹

¹European Organization for Nuclear Research (CERN), Switzerland

²Technische Universität Wien, Austria

³CEA Irfu, Université Paris-Saclay, F-91191 Gif-sur-Yvette, France

⁴CENBG, CNRS/IN2P3-Université de Bordeaux, Gradignan, France

⁵CEA, DAM, DIF, F-91297 Arpajon, France

⁶European Commission, Joint Research Centre, Geel, Retieseweg 111, B-2440 Geel, Belgium

⁷Charles University, Prague, Czech Republic

⁸CEA, DEN, Cadarache, France

⁹University of Lodz, Poland

¹⁰Institut de Physique Nucléaire, CNRS-IN2P3, Univ. Paris-Sud, Université Paris-Saclay, F-91406 Orsay Cedex, France

¹¹Centro de Investigaciones Energéticas Medioambientales y Tecnológicas (CIEMAT), Spain

¹²Istituto Nazionale di Fisica Nucleare, Sezione di Bari, Italy

¹³University of Manchester, United Kingdom

¹⁴Department of Physics, Faculty of Science, University of Zagreb, Zagreb, Croatia

¹⁵University of York, United Kingdom

¹⁶University of Santiago de Compostela, Spain

¹⁷Universitat Politècnica de Catalunya, Spain

¹⁸Universidad de Sevilla, Spain

¹⁹INFN Laboratori Nazionali del Sud, Catania, Italy

²⁰Dipartimento di Fisica, Università degli Studi di Bari, Italy

²¹Instituto de Física Corpuscular, CSIC - Universidad de Valencia, Spain

²²Paul Scherrer Institut (PSI), Villigen, Switzerland

²³Instituto Superior Técnico, Lisbon, Portugal

²⁴Joint Institute for Nuclear Research (JINR), Dubna, Russia

²⁵Goethe University Frankfurt, Germany

²⁶Horia Hulubei National Institute of Physics and Nuclear Engineering, Romania

²⁷Japan Atomic Energy Agency (JAEA), Tokai-mura, Japan

²⁸Karlsruhe Institute of Technology, Campus North, IKP, 76021 Karlsruhe, Germany

²⁹National Technical University of Athens, Greece

³⁰School of Physics and Astronomy, University of Edinburgh, United Kingdom

³¹Agenzia nazionale per le nuove tecnologie (ENEA), Bologna, Italy

³²Istituto Nazionale di Fisica Nucleare, Sezione di Bologna, Italy

³³Dipartimento di Fisica e Astronomia, Università di Bologna, Italy

³⁴Physikalisch-Technische Bundesanstalt (PTB), Bundesallee 100, 38116 Braunschweig, Germany

³⁵Istituto Nazionale di Fisica Nucleare, Sezione di Legnaro, Italy

³⁶Consiglio Nazionale delle Ricerche, Bari, Italy

³⁷Istituto Nazionale di Fisica Nucleare, Sezione di Trieste, Italy

³⁸Dipartimento di Fisica e Astronomia, Università di Catania, Italy

³⁹University of Ioannina, Greece

⁴⁰University of Vienna, Faculty of Physics, Vienna, Austria

⁴¹University of Granada, Spain

⁴²Department of Physics, University of Basel, Switzerland

⁴³Centre for Astrophysics Research, University of Hertfordshire, United Kingdom

⁴⁴Bhabha Atomic Research Centre (BARC), India

⁴⁵Australian National University, Canberra, Australia

Abstract. ^{233}U is the fissile nuclei in the Th-U fuel cycle with a particularly small neutron capture cross section which is on average about one order of magnitude lower than its fission cross section. Hence, the measurement of the $^{233}\text{U}(n,\gamma)$ cross section relies on a method to accurately distinguish between capture and fission γ -rays. A measurement of the ^{233}U α -ratio has been performed at the n_TOF facility at CERN using a so-called fission tagging setup, coupling n_TOF's Total Absorption Calorimeter with a novel fission chamber to tag the fission γ -rays. The experimental setup is described and essential parts of the analysis are discussed. Finally, a preliminary ^{233}U α -ratio is presented.

1 Introduction

The Th-U fuel cycle [1, 2] poses an alternative to the U-Pu fuel cycle for nuclear power, thus its relevant cross-sections have to be accurately known. The α -ratio is defined as the ratio between the capture and fission cross section of an isotope. The fission cross section of ^{233}U is well known but the available data for the $^{233}\text{U}(n,\gamma)$ cross section are scarce [3]. The reason is that the $^{233}\text{U}(n,f)$ cross section is on average one order of magnitude larger, as shown in Figure 1. Therefore, the measurement of the $^{233}\text{U}(n,\gamma)$ cross section relies on an efficient discrimination of the fission γ -rays from the capture events. Coupling a γ -ray detector with a fission detector allows to tag the γ -rays from fission and efficiently subtract them from the total measured spectra. A similar technique was used in several experiments [4–8].

2 Experimental Setup

2.1 The n_TOF facility

The neutron Time-Of-Flight facility n_TOF at CERN was proposed [9] and offers two beam lines for neutron cross-section measurements. The measurement of the ^{233}U α -ratio was performed in the first experimental area (EAR1) [10] of n_TOF with a flight path length of 185 m. At n_TOF neutrons are produced by spallation reactions induced by a 20 GeV/c pulsed proton beam from the CERN Proton Synchrotron on a water-cooled lead target. The fast neutrons created in the spallation process are moderated in a 4 cm layer of borated light water, eventually covering neutron energies from thermal up to few GeV.

2.2 The Total Absorption Calorimeter

The γ -ray cascades emitted in the capture reaction are detected by n_TOF's Total Absorption Calorimeter TAC [11]. The TAC is a segmented 4π scintillator array consisting of 40 individual BaF_2 crystals. The detectors are mounted in a honeycomb structure which holds the full spherical detector shell. The shell has a 20 cm and 50 cm inner and outer diameter respectively, covering 95% of the total solid angle. In order to minimize the neutron sensitivity of the TAC, a combination of neutron moderator and absorber material is used to surround the sample. The so-called neutron absorber is made of polyethylene loaded with 7.56 w% natural lithium with a total density of 1.06 g/cm^3 and is shown in Figure 2. The data acquisition system is based on digitizers and the waveforms are analyzed offline, grouped together using a coincidence window of 12 ns. Each of those TAC events is characterized by its time-of-flight

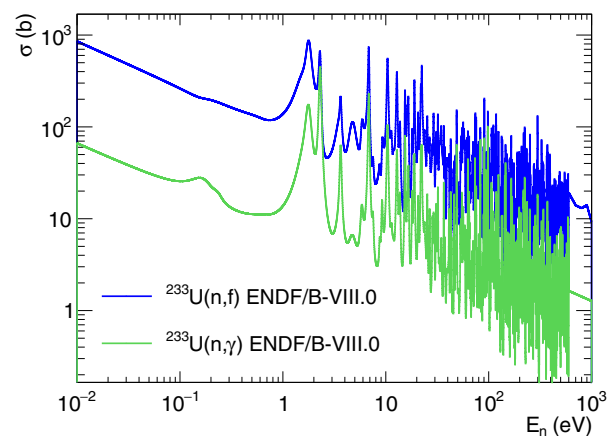


Figure 1. Comparison of fission and capture cross section from the ^{233}U evaluation of ENDF/B-VIII.0

*e-mail: michael.bacak@cern.ch

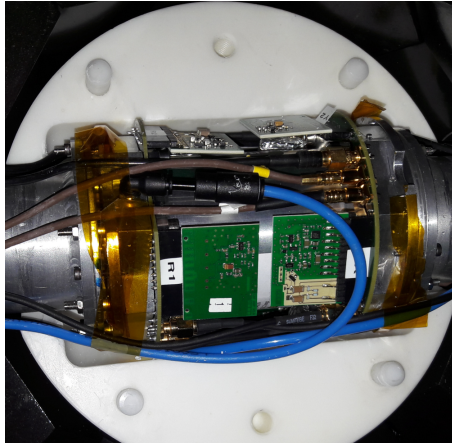


Figure 2. FICH fully connected and integrated into the absorber of the TAC.

TOF, determining the neutron energy E_n , the total deposited energy in the TAC E_{Sum} , and the number of hit crystals m_{cr} . The main advantage of the TAC is the use of those quantities to discriminate between different types of reactions, for example ambient background and γ -ray cascades from the (n,γ) process.

2.3 The compact fission chamber

In order to properly tag and remove the main source of γ -background, namely the prompt γ -ray cascades of the $^{233}\text{U}(n,f)$ reaction from the total measured spectra, a fission chamber (*FICH*) [12] has been developed. The detector is designed as a multi-plate ionization chamber containing two stacks of axial ionization cells. Figure 2 shows a picture of the FICH fully assembled and mounted in the neutron absorber. With a total length of 120 mm and a diameter of 90 mm the chamber hosts 14 ionization cells. Each cell has an inter-electrode gap of 3 mm which is not sufficient to stop fission fragments exiting perpendicular from the sample, but allows better timing performance. The detector is operated with high-purity CF_4 at a pressure of 1100 mbar controlled by a dedicated gas regulation system. Pre-amplifier and shaper modules [13] are directly mounted on the motherboards of each stack to reduce signal attenuation and to improve the signal to noise ratio.

Fourteen uranium oxide layers have been deposited at JRC-Geel on 10 μm thick aluminium foils by molecular plating. The base material was 99.936 % enriched in ^{233}U with the largest contaminant being 0.0496 % ^{234}U . The diameter of the mask used for the preparation of the ^{233}U samples was 40.00 ± 0.02 mm which also defines the active area of the samples. The activity of each sample has been determined by well-defined solid angle α -particle counting and amounts to an average α -activity of about 1.16 MBq per sample translating to an average areal mass density of $264.5 \mu\text{g}/\text{cm}^2$.

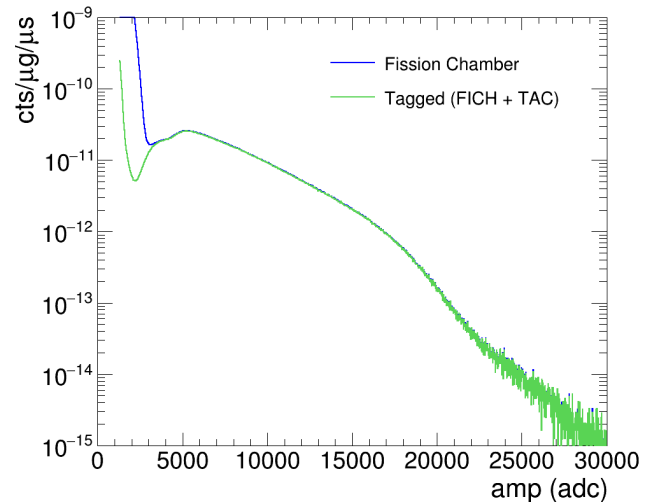


Figure 3. Comparison of the amplitude spectrum of the FICH and tagged signals.

3 Experimental response to $^{233}\text{U} + n$ events

The event reconstruction of fission tagged events was performed by setting a constant coincidence window of 14 ns between TAC and FICH events. The amplitude spectra of the events from the fission chamber and from tagged events is shown in Figure 3. The reduction of the α -particle background from the natural decay of ^{233}U is clearly visible, allowing for a cleaner α -FF separation.

3.1 FICH Efficiency

A critical part in the analysis concerns the calculation of the detection efficiency of the fission chamber ε_{FICH} which is based on the assumption that a fission event is detected independently by the TAC and the FICH. In this case, the fission chamber efficiency ε_{FICH} can be calculated solely from the experimental data. For fission events with amplitudes larger than 3000 adc channels the efficiency has a value of 0.867 ± 0.002 . A more detailed description can be found in [14].

3.2 Background subtraction

In order to obtain the shape of the TAC response to $^{233}\text{U}(n,\gamma)$ events from the total measured sum energy spectra all background components have to be carefully subtracted. Dedicated measurements have been carried out to determine the contributions of the fission chamber without the ^{233}U layers (*Dummy*), the ambient background and the background induced by the natural α -activity of the radioactive isotopes in the samples. The *prompt fission γ -ray* spectrum is obtained by fission tagging and has to be corrected for the detection efficiency of the fission chamber ε_{FICH} . The sum energy spectra of the different contributions are compared to the total measured

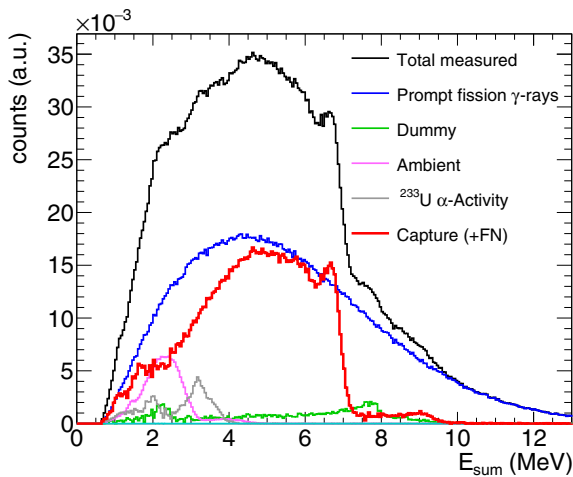


Figure 4. Components of the total measured deposited energy spectrum for a neutron energy range of $2.2\text{ eV} < E_n < 2.4\text{ eV}$ and $m_{cr} \geq 3$.

spectrum in Figure 4 in the strongest capture resonance corresponding to a neutron energy range of $2.2\text{ eV} < E_n < 2.4\text{ eV}$ and for events with $m_{cr} \geq 3$ in order to clean the low crystal multiplicity background which would otherwise dominate the region for $E_{Sum} < 1.5\text{ MeV}$. After subtraction of the various background contributions the shape of the TAC response to $^{233}\text{U}(n,\gamma)$ events becomes visible. A sum peak appears at $E_{Sum} \approx 6.85\text{ MeV}$ corresponding to the neutron separation energy of ^{234}U .

The shape of the remaining background in the *Capture* component above $E_{Sum} = 7.5\text{ MeV}$ does not match any other background component, leading to the conclusion that there is some other source of background not accounted for. The most probable explanation is related to the prompt fission neutrons (*FN*) being moderated and captured in the experimental setup. This shape is peculiar to the TAC as it shows the sum energy peaks at the separation energy of the main barium isotopes due to fission neutrons captured in the barium nuclei of the BaF_2 crystals within the first few microseconds after emission. Gating, for example, on the first micro second after a fission event allows to determine the shape of this FN background component. In Figure 5 the shape of the background induced by fission neutrons is compared to the background induced by neutron scattering in the range of $2.2\text{ eV} < E_n < 2.4\text{ eV}$, measured with a carbon sample. The two spectra show similar capture reactions characterized by the different sum energy peaks but with different intensities resulting in completely different shapes. Specifically the neutron separation energy of $^{135}\text{Ba}+n$ corresponding to the sum energy peak at $E_{Sum} = 9.1\text{ MeV}$ is strongly suppressed in the scattered neutron spectra compared to the FN spectrum. Therefore, the scattered neutron spectrum cannot explain the remaining background in the *Capture* com-

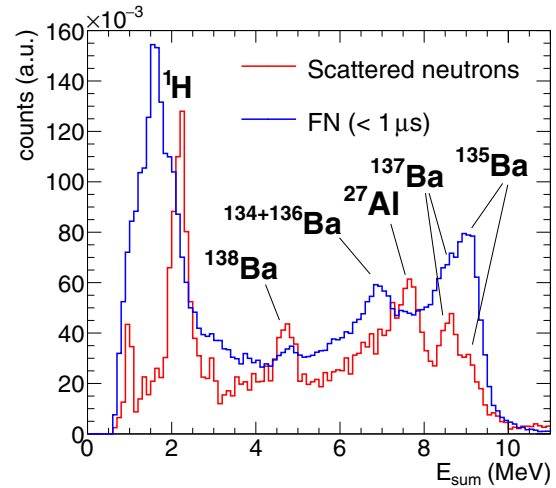


Figure 5. Comparison of the fission neutron and neutron scattering spectrum for a neutron energy range of $2.2\text{ eV} < E_n < 2.4\text{ eV}$. The sum energy peaks are labeled with nucleus X corresponding to the neutron separation energy of the nucleus after capture $X + n$.

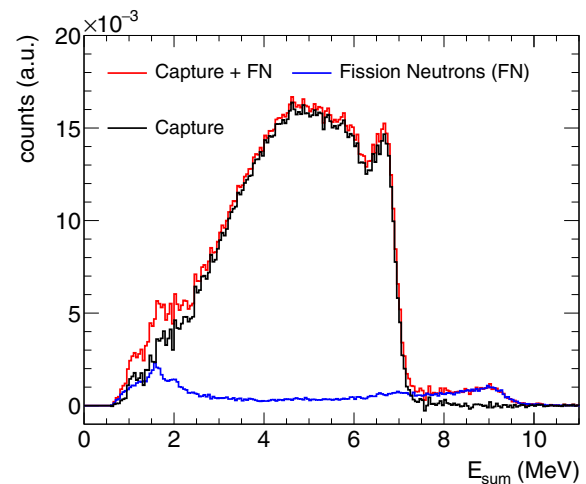


Figure 6. Subtraction of the contribution from fission neutrons in the neutron energy range of $2.2\text{ eV} < E_n < 2.4\text{ eV}$.

ponent in Figure 4 above $E_{Sum} = 7.5\text{ MeV}$. However, the FN background component matches the shape of the remaining background above $E_{Sum} = 7.5\text{ MeV}$ as shown in Figure 6, indicating that this background is related to fission neutrons. The FN component scales with the fission cross section allowing for an accurate correction and its contribution to the remaining capture response is shown in Figure 6.

4 Determination of the ^{233}U α -ratio

Following the background subtraction, the efficiency of detecting the γ -ray cascades with the TAC has been calculated using the Monte Carlo simulation toolkit

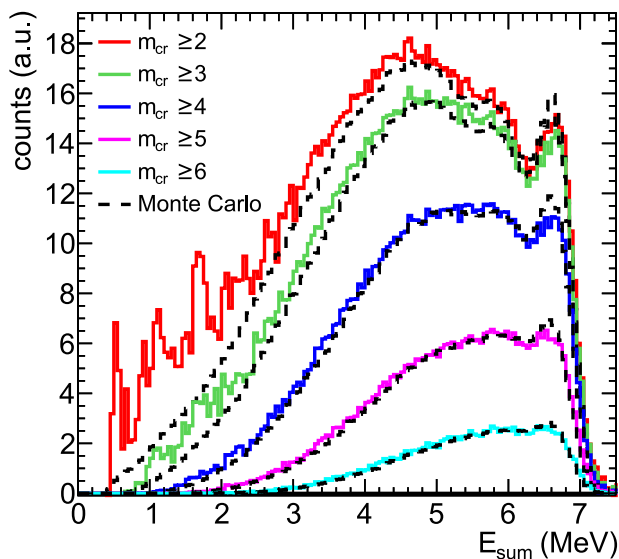


Figure 7. Comparison of the experimental and simulated response to $^{233}\text{U}(n,\gamma)$ events.

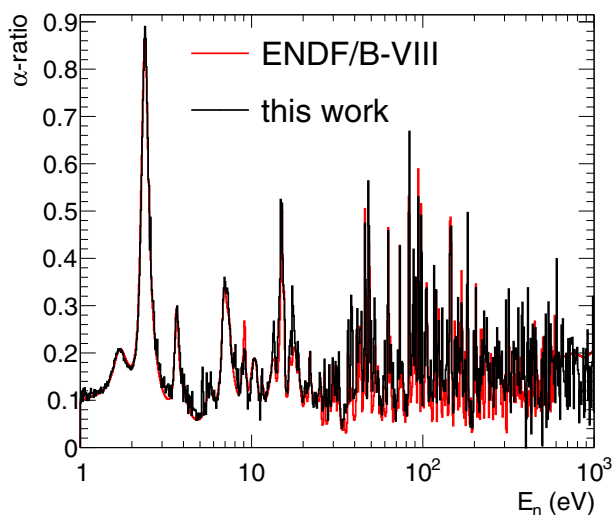


Figure 8. Preliminary ^{233}U α -ratio for $1\text{ eV} < E_n < 1\text{ keV}$ compared to ENDF/B-VIII.0.

Geant4 [15]. The whole experimental setup, including the TAC, FICH, absorber and beam pipes has been modelled in Geant4.

The cascades emitted in the $^{233}\text{U}(n,\gamma)$ process were simulated with DICEBOX [16] and a comparison between the experimental and simulated response to $^{233}\text{U}(n,\gamma)$ events can be seen in Figure 7. The overall agreement for crystal multiplicities $m_{cr} \geq 3$ is good and allows to calculate the capture efficiency for a given analysis cut. The contribution of the isomeric states in the fission products (absent in the simulations) is important for events with $m_{cr} \geq 2$ and $E_{Sum} < 2.5\text{ MeV}$. With a preliminary estimation of the detection efficiency of $(76.2 \pm 2.2)\%$ for $m_{cr} \geq 3$ and $2.5\text{ MeV} < E_{Sum} < 7\text{ MeV}$ the ^{233}U α -ratio can be calculated from the response of the FICH and the

TAC. In Figure 8 the preliminary result of the ^{233}U α -ratio measurement is compared to the ^{233}U α -ratio of the ENDF/B-VIII database. Overall, the ratios are in good agreement and local deviations are under investigation.

5 Summary

A fission tagging experiment to determine the ^{233}U α -ratio has been performed at n_TOF EAR1 yielding promising results for neutrons from thermal energies to several keV. The experimental setup and the key elements from the analysis have been described and a preliminary ^{233}U α -ratio has been presented. A detailed analysis of the extracted ^{233}U α -ratio is currently being performed and will be published in a forthcoming paper.

This work was partially supported by the French NEEDS/NACRE Project and by the European Commission within HORIZON2020 via the EU-RATOM Project EUFRAT. The authors would like to acknowledge more specifically JRC Geel for targets preparation and for providing full support for a first test measurement of the fission chamber at GELINA.

References

- [1] V.G. Pronyaev, IAEA Report INDC (NDS) **408**, (1999)
- [2] The Generation IV International Forum, <http://www.gen-4.org/> (2013)
- [3] L. W. Weston et al., Nuc. Sc. Eng. **34**:1, 1-12 (1968)
- [4] C. Guerrero, E. Berthoumieux et al., Eur. Phys. J. A **48**, 29 (2012)
- [5] J. Balibrea-Correa et al., EPJ Web of Conf. **146**, 11021 (2017)
- [6] J. Balibrea-Correa, *Measurement of the neutron capture cross section of ^{235}U at the n_TOF facility*, PhD thesis, Madrid (2017)
- [7] M. Jandel et al., Phys. Rev. Lett. **109**, 202506 (2012)
- [8] S. Mosby et al., Phys. Rev. C **89**, 034610 (2014)
- [9] C. Rubbia et al., CERN/LHC/98-02; CERN: Geneva, Switzerland (1998)
- [10] C. Guerrero et al., Eur. Phys. J. A **49**, 27 (2013)
- [11] C. Guerrero et al., Nucl. Instr. Meth. A **608**, 424 (2009)
- [12] M. Bacak et al., EPJ Web Conf. **146**, 03027 (2017)
- [13] J. Taieb et al., Nucl. Instr. Meth. A **833**, 1 (2016)
- [14] M. Bacak et al., EPJ Web Conf. **211**, 03007 (2019)
- [15] S. Agostinelli et al., Nucl. Instr. Meth. A **506**:250–303 (2003)
- [16] F. Bečvář, Nucl. Instr. Meth. A **417**, 434 (1998)